Superior Photochromic Performance of Naphthopyrans in a Rigid Host Matrix Using Polymer Conjugation: Fast, Dark, and Tunable

Nino Malic,[†,||] Jonathan A. Campbell,[§,||] and Richard A. Evans*[,†,‡,||]

CSIRO Molecular & Health Technologies, Bag 10, Clayton VIC 3169 Australia, Centre of Advance Macromolecular Design, School of Chemical Sciences and Engineering and School of Chemical Sciences and Engineering, The University of New South Wales, Sydney, NSW, 2052, Australia, and The Cooperative Research Centre for Polymers, 8 Redwood Drive, Notting Hill, VIC 3168, Australia

Received August 8, 2007; Revised Manuscript Received December 3, 2007

ABSTRACT: The attachment of low T_g poly(*n*-butyl acrylate) polymers (M_n 4100 to 13 100) to naphthopyran photochromic dyes provided large tunable improvements in their photochromic performance in a rigid thermoset host polymer matrix. Both coloration and decoloration speeds were greatly increased, with the critical $t_{1/2}$ decoloration times reduced by 50−95% and $t_{3/4}$ decoloration times reduced by at least 63% through the use of these polymer conjugates. In addition, the optical density of the colored form of the dye−polymer conjugates rapidly reached a steady state absorption ca. 60−70% greater than the nonpolymer conjugated control dyes. The effect of the geometry of the polymer conjugates was examined, and it was found that mid-placement of the dye on the polymer provided secondary decoloration speed enhancement over end-placement. Thus, conjugation of low T_g poly(*n*-butyl acrylate) not only provides faster coloration and decoloration but also greatly increases optical density with near square-wave characteristics.

Introduction

Traditionally, the main interest in photochromic dyes and their materials has been in their ability to undergo reversible color change for either ophthalmic or optical data storage applications.[1−6] However, there is increasing interest in the use of such systems to modulate conductivity, fluorescence, magnetism, and cellular adhesion as described in a recent review.[7] Common to many of these and new applications is the conjugation of photochromic dyes to polymers,[7−20] and this includes their use in photochromic lenses which remains, by a wide margin, the largest commercial application of conventional photochromic dyes in general. Accordingly, the understanding and control of the switching performance of photochromic dyes with polymers and specifically within rigid polymeric matrices have been important areas of research. Ongoing efforts in this area have focused largely on increasing switching speeds, particularly decoloration. Some methods which have been explored are the changing of the electronic properties of the dye itself, i.e., to synthesize a dye that is inherently fast,[21−23] and modification of the host matrix in which the dye is incorporated.[24−27] Both of these methodologies have their compromises. Electronic and structural modifications are relatively unpredictable in their effectiveness, and matrix modification can compromise the mechanical properties.

A new approach in controlling photochromic switching performance within rigid cross-linked polymer matrices has recently been realized through the development of photochromic dye−polymer conjugates. Since our initial publication[11] describing the use of living radical polymerization techniques with photochromic moieties, other researchers have found the combination useful for their photochromic applications.[16,17] We have used the living radical polymerization and other methods to show the utility of attaching a single photochromic dye to a single polymer chain to control the photochromism of the dye.[8−11,13] The work showed that the covalent attachment of a polymer directly to a dye allows for the control of the immediate local environment surrounding each individual dye molecule or their aggregates without compromising the properties of the bulk polymeric matrix in which it is contained.

The ability of spirooxazine and naphthopyran (chromene) dyes to switch between their colored and uncolored forms is greatly affected by the viscosity of their medium since the switching requires a physical mechanical motion, where half the molecule undergoes an approximate 90° rotation (Figure 1). Thus, placement of the dye in a rigid cross-linked host matrix represents the most severe test of a dye's photochromic performance. Having a highly localized fluid environment around the dye by conjugating a soft oligomer/polymer allows for greater freedom of movement for this motion to occur, resulting in faster switching.[8]

A particular facet of this technique was demonstrated by using atom transfer radical polymerization (ATRP) to grow polymers of well-controlled molecular weight and polydispersity from a photochromic spirooxazine macroinitiator.[11,13] Having a high T_g polymer attached to the dye, such as polystyrene and poly(methyl methacrylate), retarded switching rates. Providing a fluid environment surrounding the dye via the attachment of a low T_g polymer, namely, poly(*n*-butyl acrylate), dramatically accelerated the switching performance of the spirooxazines.[13]

Naphthopyrans are an important commercial class of photochromic dyes due to their good fatigue properties and strongly colored state while representing the best source of yellow and red colors.[28−31] To date, no polymer conjugation of free radically derived polymers to naphthopyrans in this manner or their photochromic performance has been reported. We now report the synthesis of mid- as well as end-functionalized 2,2-diaryl-2*H*-naphtho[1,2-*b*]pyran dye−poly(*n*-butyl acrylate) conjugates and the highly beneficial effect this conjugation has on the

* Email: richard.evans@csiro.au.
† CSIRO Molecular & Health Technologies.
‡ Centre of Advance Macromolecular Design, The University of New South Wales.
§ School of Chemical Sciences and Engineering, The University of New South Wales.
|| The Cooperative Research Centre for Polymers.

10.1021/ma071792l CCC: $40.75
Published on Web 01/24/2008

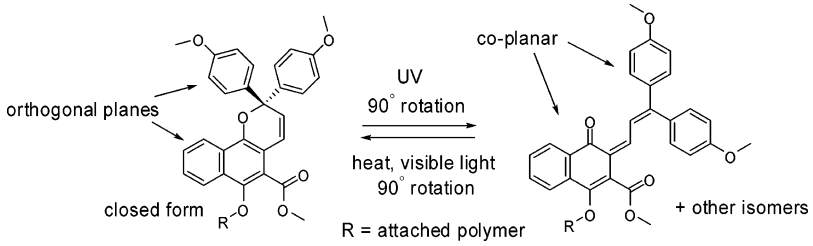

Figure 1. Transitions between the closed and open forms of a 2,2-diaryl-2*H*-naphtho[1,2-*b*]pyran illustrating the mechanical rotation of the bulky *gem*-diaryl substituents.

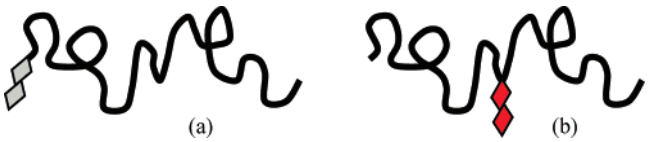

Figure 2. Photochromic dye−polymer conjugates, where attachment of the dye is at the (a) end and (b) middle of the polymer. Structure (b) is expected to provide better dye encapsulation per unit length of attached polymer when incorporated within rigid polymeric matrices.

photochromism on the naphthopyran. In addition, we also studied the effect of where the dye was placed on the polymer. This was achieved through our recently published methodology for the synthesis of Y-branched polymeric tail architectures via ATRP and RAFT polymerization, which allows for the facile synthesis of mid-functionalized polymer conjugates.[32]

It is expected that for a given molecular weight of polymer the attachment of the dye to the middle of the polymer would provide more efficient encapsulation than the placement at the end (Figure 2). Specifically, dyes would switch faster when placed in the middle of a low T_g polymer than at the end. As a result of more efficient polymer encapsulation via mid-polymer attachment of the dye, the molecular weight of the polymer conjugated to the dye needed for a given switching speed can be reduced.

Results and Discussion

The napthopyran selected for examination, **8**, is of the class described by Van Gemert et al.[33] in their patent. It is relatively straight forward to synthesize[33,34] and possesses a free hydroxyl group that is readily functionalized with our initiator systems. The 6-acetoxy analogue of **8** has been previously shown to have very slow switching kinetics when incorporated within a rigid sol−gel prepared gel−glass matrix.[35] The naphthopyran selected gives a red colored isomer (λ_{max} ca. 510 nm) on UV irradiation.

The synthesis of mid-functionalized photochromic dye−polymer conjugates is enabled through the use of a Y-branching linker. We have previously documented a facile water based synthesis of functionalized macroinitiators containing two ATRP initiating moieties from the useful synthon 3,5-dihydroxybenzoic acid, **2**.[32] Reaction of **2**, in cold and basic water−isopropanol solution, with 2 equiv of 2-bromoisobutyryl bromide **3a** gave the bisacylated product **6a** in 75% yield. Conversion to the acid chloride **7a** was achieved using thionyl chloride and DMF as the catalyst. Subsequent reaction with the hydroxyl-functionalized naphthopyran **8** gave the bisfunctionalized ATRP macroinitiator **10a** (Scheme 1).

The synthesis of the monofunctionalized ATRP macroinitiator **9a** was achieved in the same way as for **10a**, however, using 3-hydroxybenzoic acid **1** as a linking group. For the purpose of an accurate comparison, we used such a linker in order to replicate, as best possible, any effects resulting from the steric bulk of the Y-branching linker of the bis-system. Reaction of **1** with acid bromide **3a** gave the acylated derivative **4a** in 98% yield, which was then quantitatively converted to the acid chloride **5a** and reacted with naphthopyran **8** to give the monofunctionalized ATRP macroinitiator **9a**.

The naphthopyran derivatives **9b** and **10b** (control compounds) were synthesized in an identical manner as that of the macroinitiators **9a** and **10a**, using the non-brominated acid halide **3b**. Once again, these control compounds were synthesized to contain functionalized (di)hydroxybenzoic acid moieties to replicate as close as possible the steric bulk of the linker groups of both systems.

Polymerizations using the naphthopyran macroinitiators **9a** and **10a** were performed under homogeneous ATRP conditions with CuBr and 4,4′-dinonyl-2,2′-bipyridine functioning as the catalyst system (Scheme 1). This method has been used previously and has been shown to be effective in forming poly(*n*-butyl acrylate)-spirooxazine conjugates with well-controlled properties.[13] As with this previous study, here, we also see polymerization characteristics which are indicative of good living behavior, namely, consistently low polydispersities (∼1.10) and a linear growth of molecular weight (M_n) with conversion. Details of polymer conjugates **11a**−**d** and **12a**−**c** are summarized in Table 1.

The polymerizations giving end-functionalized conjugates **11a**−**d** were conducted with an *n*-butyl acrylate to **9a** ratio of 100:1. Figure 3 shows a slight deviation of the molecular weights from those of the theoretical values, which could be attributed to a lower than expected initiator efficiency as well as the presence of high molecular weight products arising from chain termination via radical coupling. The presence of such radical coupled products was confirmed by GPC analysis which showed a small shoulder on the main peak toward higher molecular weight. The shoulder became more prominent at higher conversions and is a common characteristic of living radical polymerizations by ATRP. In contrast, polymerizations giving mid-functionalized conjugates **12a**−**c** were conducted with an *n*-butyl acrylate to **10a** ratio of 200:1 (Figure 4). This was done to compensate for the presence of two ATRP initiating moieties (2-bromoisobutyryl esters) per macroinitiator molecule, **10a**, thus effectively maintaining a 100:1 molar ratio of monomer to initiator. A halving of this ratio would see a greater proportion of chain termination, resulting from intermolecular and intramolecular radical coupling. Intramolecular radical coupling giving dead cyclic polymer chains is a phenomenon previously observed in the ATRP polymerization of *n*-butyl acrylate using a similar type of Y-branched macroinitiator.[32] Not unexpectedly, a small proportion of both these types of termination products were observed on analysis of the product conjugates by GPC, with a progressively greater proportion being observed at higher conversions. This is indicated by the presence of shoulders on both sides of the main peak in the GPC trace (see Supporting Information).

A comparison of the ^{1}H NMR spectrum of a low molecular weight mid-functionalized poly(*n*-butyl acrylate)−naphthopyran

Scheme 1. Synthesis Scheme for Photochromic ATRP Macroinitiators 9a and 10a, Control Compounds 9b and 10b, and *n*-Butyl Acrylate Polymerizations Giving Dye−Polymer Conjugates 11a−d and 12a−c

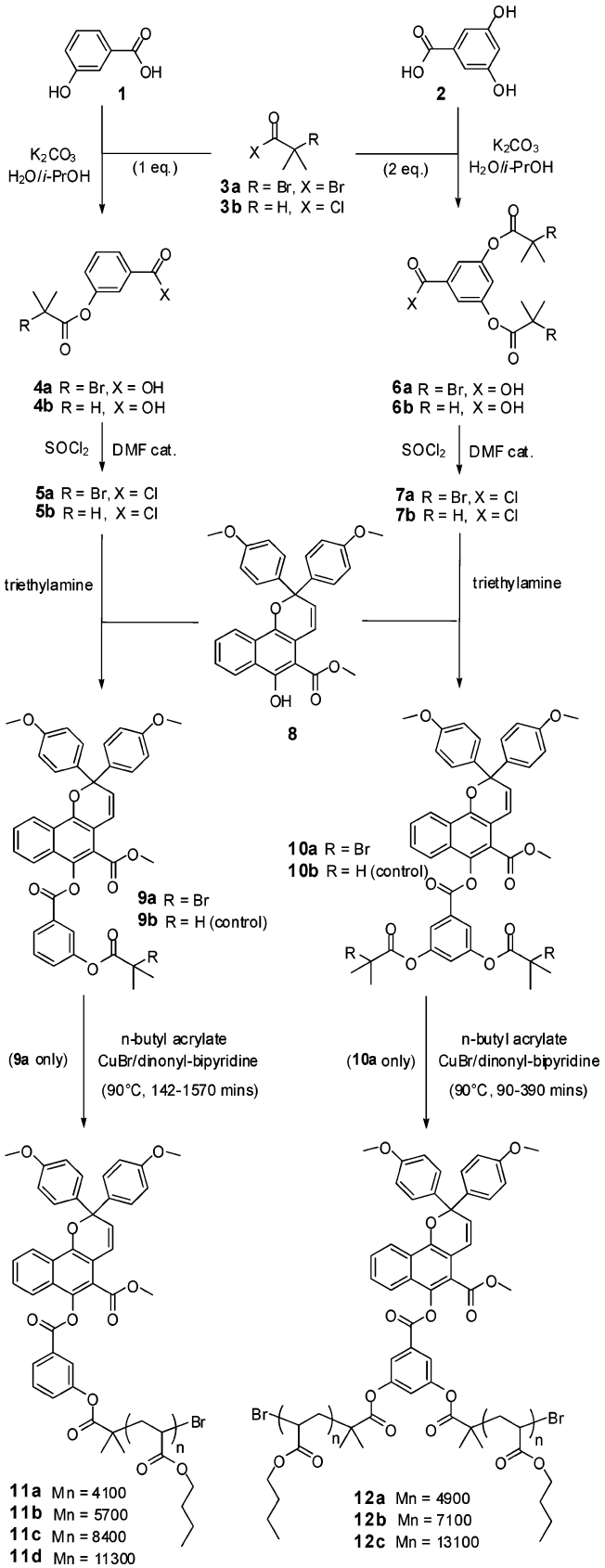

conjugate, **12a**, along with the naphthopyran macroinitiator **10a** from which it was derived is given in Figure 5. The peaks corresponding to the naphthopyran photochromic moiety

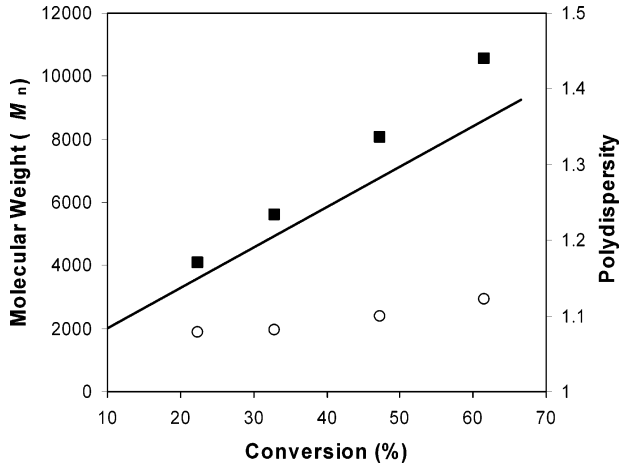

Figure 3. Evolution of molecular weight (■) and polydispersity (○) of conjugates **11a−d** during atom transfer radical polymerization (ATRP) of *n*-butyl acrylate using macroinitiator **9a**, where [*n*-butyl acrylate]:[CuBr]:[dinonyl-bipyridine]:[**9a**] = 100:1:2:1.

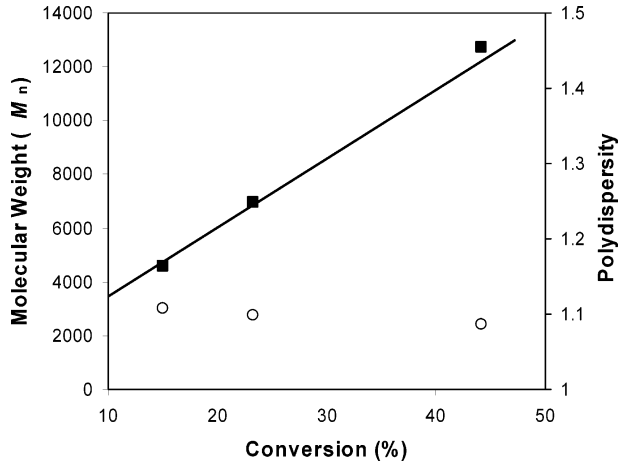

Figure 4. Evolution of molecular weight (■) and polydispersity (○) of conjugates **12a−c** during atom transfer radical polymerization (ATRP) of *n*-butyl acrylate with macroinitiator **10a**, where [*n*-butyl acrylate]:[CuBr]:[dinonyl-bipyridine]:[**10a**] = 200:1:2:1.

Table 1. Polymerization Characteristics of Poly(*n*-butyl acrylate)−Naphthopyran Dye Conjugates 11a−d and 12a−c (Scheme 1) Using Naphthopyran Macroinitiators 9a and 10a

sample	polymerization duration (min)[a]	conversion (%)[b]	exptl M_n[c]	calcd M_n[d]	PDI
11a	270	22.3	4100	3596	1.08
11b	491	32.8	5600	4942	1.08
11c	965	47.3	8000	6800	1.10
11d	1570	61.5	10 600	8620	1.12
12a	90	15.0	4600	4745	1.11
12b	140	23.3	6900	6872	1.10
12c	390	44.2	12 700	12 230	1.09

[a] Polymerizations for **11a− d** were performed at 90 °C with *n*-butyl acrylate (15.60 mmol), macroinitiator **9a** (0.156 mmol), 4,4′-dinonyl-2,2′-bipyridine (0.312 mmol), and CuBr (0.156 mmol) in benzene (3 mL) solution. Polymerizations for **12a−c** were similarly performed, however, using 31.21 mmol *n*-butyl acrylate and 2 mL benzene. [b] Determined by ^{1}H NMR analysis of reaction mixture in d_6-acetone solution. [c] Determined by GPC analysis (polystyrene calibration standards) of unpurified polymer conjugates. [d] Calculated based on monomer conversion plus macroinitiator molecular weight.

are clearly visible in the spectrum of the conjugate. Signals from the two CH_3O groups of the substituted *gem*-diphenyls and the CH_3 of the ester moiety on the naphthyl group overlap at 3.78 ppm. The aromatic region shows naphthyl protons at 8.46, 7.91, 7.71, and 7.63 ppm, *p*-methoxy substituted

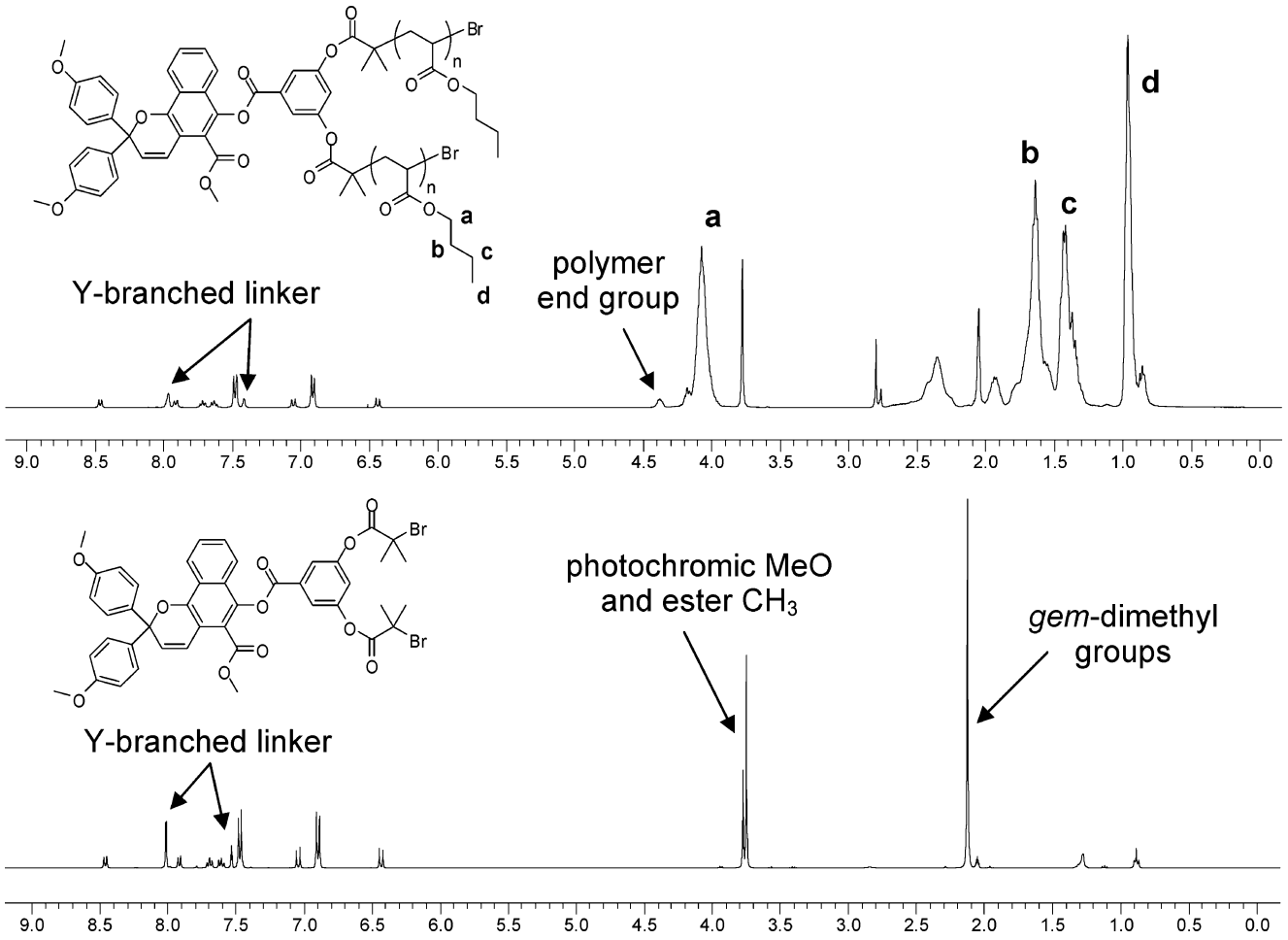

Figure 5. Comparison between ^{1}H NMR spectra (d_6-acetone) of mid-functionalized poly(*n*-butyl acrylate)−naphthopyran conjugate **12a** (top) and the corresponding naphthopyran-functionalized macroinitiator **10a** (bottom).

Table 2. Photophysical Analysis of the Decoloration of Poly(*n*-butyl acrylate)−Naphthopyran Conjugates Relative to Control Compounds 9b and 10b in a Poly(ethylene glycol) 400 Dimethacrylate (PEGDMA)/2,2′-Bis((4-methacryloxyethoxy)phenyl)propane (EBPDMA) Test Lens[a]

sample	M_n[b] (PD)	$t_{1/2}$[c]	$t_{3/4}$[c]	A_0	k_1 (min^{-1})	A_1	k_2 (min^{-1})	A_2	A_{th}
9b	control	139	2131	1.07	0.85	0.50	0.06	0.23	0.22
11a	4100 (1.08)	70	782	1.70	1.20	0.58	0.07	0.18	0.20
11b	5700 (1.07)	52	545	1.77	1.44	0.63	0.08	0.15	0.19
11c	8400 (1.08)	39	410	1.80	1.82	0.68	0.09	0.12	0.18
11d	11300 (1.09)	37	308	1.44	1.85	0.67	0.09	0.12	0.18
10b	control	263	n/a	1.01	0.77	0.41	0.05	0.26	0.27
12a	4900 (1.09)	46	636	1.73	1.68	0.61	0.08	0.16	0.19
12b	7100 (1.09)	32	322	1.72	2.15	0.67	0.09	0.12	0.18
12c	13 100 (1.07)	21	104	1.75	2.96	0.75	0.10	0.08	0.17

[a] Samples initially irradiated at 350−400 nm for 1000 s and then decoloration monitored at λ_{max} of the colored form of the naphthopyran dye (510 nm) at 20 °C in the dark for a further duration of 4800 s (maximum). [b] Molecular weight (M_n) of conjugates post purification from GPC analysis using polystyrene calibration. [c] Time taken to reach one-half ($t_{1/2}$) and three-quarters ($t_{3/4}$) of the initial absorbance. Values are averages of 3 runs per lens sample.

gem-diphenyl protons as two doublets at 7.48 and 6.91 ppm, olefinic protons of the pyran ring as two doublets at 7.05 and 6.44 ppm, and signals for protons of the linker group as singlets at 7.96 and 7.41 ppm, which are shifted upfield from 8.01 and 7.52 ppm when compared with the macroinitiator **10a**. This shifting of signals is due to the movement of the Br atoms away from the linker upon polymerization. The end groups of the polymer are visible as a signal at 4.38 ppm corresponding to CHBr. The displacement of the Br atoms is also reflected in the shifting of the *gem*-dimethyl signals of the 2-bromoisobutyryl moieties of the macroinitiator from 2.12 ppm. The signal is no longer visible in the spectrum of the polymer conjugate as it is expected to reside beneath the signals of the bulk polymer between 1 and 2 ppm. A comparison of the two spectra gives a good indication of the successful synthesis of conjugates having the structure depicted in Scheme 1.

Each poly(*n*-butyl acrylate)−naphthopyran dye conjugate and the control compounds **9b** and **10b** were added to the methacrylate based host matrix of poly(ethylene glycol) 400 dimethacrylate (PEGDMA) and 2,2′-bis((4-methacryloxyethoxy)phenyl)propane (EBPDMA) (1:4 by wt) lens formulation at the same molar concentration, then added to a mould, and heat cured to give a test lens. All samples were then subjected to an identical analysis procedure: irradiation at 350−400 nm for 1000 s while monitoring the absorbance at λ_{max} of the colored form of the naphthopyran dye (510 nm) at 20 °C, then further continuous monitoring of the decoloration in the dark for a maximum of 4800 s. In contrast to the previously mentioned work of an analogous dye incorporated within a sol−gel

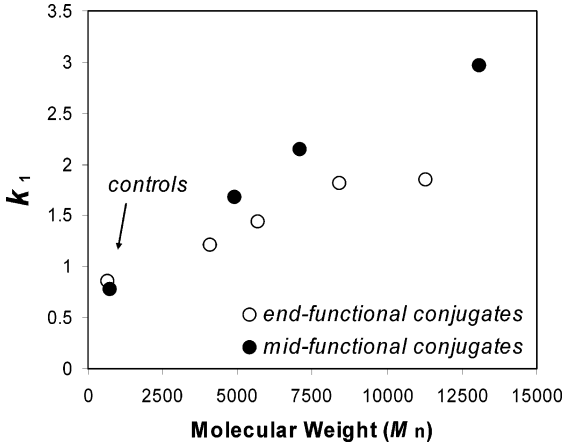

Figure 6. Decoloration of the colored form of naphthopyran after irradiation at 350−400 nm monitored at 510 nm. Evolution of k_1 (rate of decoloration, fast component) with molecular weight of naphthopyran end-functionalized poly(*n*-butyl acrylate) conjugates **11a**−**d** and control compound **9b** (○) and naphthopyran mid-functionalized poly(*n*-butyl acrylate) conjugates **12a**−**c** and control compound **10b** (●) in the host matrix PEGDMA:EBPDMA (1:4). Dye concentration = 1.20×10^{-6} mol/g.

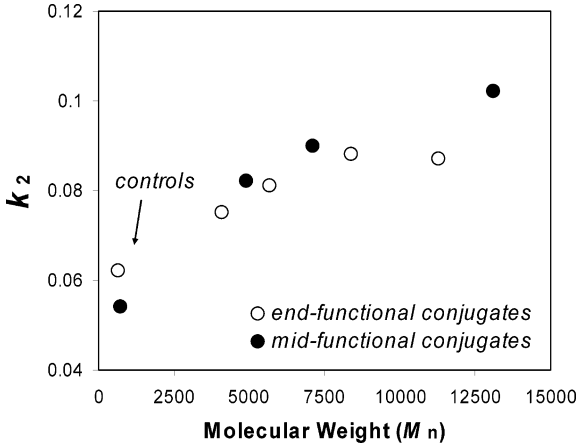

Figure 7. Decoloration of the colored form of naphthopyran after irradiation at 350−400 nm monitored at 510 nm. Evolution of k_2 (rate of decoloration, slow component) with molecular weight of naphthopyran end-functionalized poly(*n*-butyl acrylate) conjugates **11a**−**d** and control compound **9b** (○) and naphthopyran mid-functionalized poly(*n*-butyl acrylate) conjugates **12a**−**c** and control compound **10b** (●) in the host matrix PEGDMA:EBPDMA (1:4). Dye concentration = 1.20×10^{-6} mol/g.

prepared matrix,[35] the photophysical analysis of the conjugates incorporated within our rigid polymeric test lens system showed very rapid switching for both the forward reaction (coloration) as well as for the reaction back to the initial state (decoloration). For decoloration, the time taken to reach one-half and three-quarters of the initial absorbance is designated as $t_{1/2}$ and $t_{3/4}$, respectively, and is a convenient measure of the fading speed where smaller numbers indicate faster decolorations. In addition, standard biexponential kinetic parameters were calculated for the decoloration in the dark.

All poly(*n*-butyl acrylate) conjugates show far superior decoloration rates compared with the control compounds (Table 2), with the rates increasing with molecular weight of the appended polymer chains. End-functionalized conjugate **11d** faded almost 4 times faster than the control **9b** to $t_{1/2}$ and almost 7 times faster to $t_{3/4}$. More impressively, the mid-functionalized conjugate **12c** was ca. 12.5 times faster to $t_{1/2}$ compared with the control **10b**. A direct numerical comparison of the $t_{3/4}$ values could not be obtained since even after 80 min the control compound **10b** did not reach three-quarters of its initial absorbance. We may qualitatively say that this value is greater than 4800 s, which in that case is a remarkable improvement.

The decoloration curves were analyzed using the following biexponential equation:

$$A(t) = A_1 e^{-k_1 t} + A_2 e^{-k_2 t} + A_{th}$$

where $A(t)$ is the optical density at λ_{max}, A_1 and A_2 are contributions to the initial optical density A_0, k_1 and k_2 are the rates of the fast and slow components, respectively, and A_{th} is the residual coloration when time approaches infinity. The model was found to accurately fit our data, giving R values (correlation coefficients) greater than 0.99. Values of the constants for each conjugate and control compound are given in Table 2. This equation is one of the many models used to fit photochromic decoloration[15] and has been used previously to model the decoloration of spirooxazines and naphthopyrans.[13,35,36]

Comparison of the decoloration performance between the end-functionalized conjugates, **11a**−**d**, and mid-functionalized conjuagates, **12a**−**c**, (see plots of k_1 and k_2 vs molecular weight, Figures 6 and 7 respectively) shows that having the photochromic dye in the center of the low T_g poly(*n*-butyl acrylate) polymer gives improved decoloration performance per unit molecular weight. This is also clearly observed in the plots of $t_{1/2}$ and $t_{3/4}$ versus molecular weight (see Supporting Information). Previous work with end-functional spirooxazine−polymer conjugates confined within a rigid host matrix proposed a de facto or statistical encapsulation model due to the natural tendency of a polymer conjugate to coil.[8] Hence, the factors which influence photochromic performance could be controlled by the choice of the attached polymer. Here, it is proposed that having two comparable polymer chains radiating from the central functional molecule (naphthopyran dye), rather than a single chain of equivalent molecular weight, provides a further enhancement of molecular encapsulation within a rigid host matrix. This is certainly reflected in the k_1 values and in the k_2 values for molecular weights above ca. 4000. For example, the mid-placed dye−polymer conjugate **12b** has a faster k_1 than the end-functionalized **11c** (2.15 vs 1.82 min^{-1}) even though **12b** is of lower molecular weight (7100 for **12b** vs 8400 for **11c**). Similar results are seen for dye−polymer conjugate **12a**, which has a faster k_1 than the end-functionalized **11b** (1.68 vs 1.44 min^{-1}), with **12a** being also of lower molecular weight (4900 for **12a** vs 5700 for **11c**). Figure 7 shows that there may be a crossover point at a molecular weight of roughly 4000, where below this value end functionalization may become comparable or more efficient in the latter stages of decoloration. Although at these low molecular weights the decoloration speeds are better than those of the control dyes in both systems, much better performance is gained at only modestly higher molecular weights.

Interestingly, there appears to be a plateau effect with end-functional dye−polymer conjugates, where increased molecular weight above M_n 8400 shows limited or no further decoloration rate increase. This is in contrast to the mid-functionalized dye−polymer conjugates, which show no such plateau of performance with increasing molecular weight within the range tested.

Although the controls are sterically similar, the use of such linking molecules has not exactly produced two electronically identical controls. Since photochromic molecules are generally very sensitive to electronic factors, the differences in kinetic performance between the two control dyes **9b** and **10b** (Table 2) may be due to the presence of only one propionyl ester moiety in **9b** compared with two in **10b**. However, despite the possible

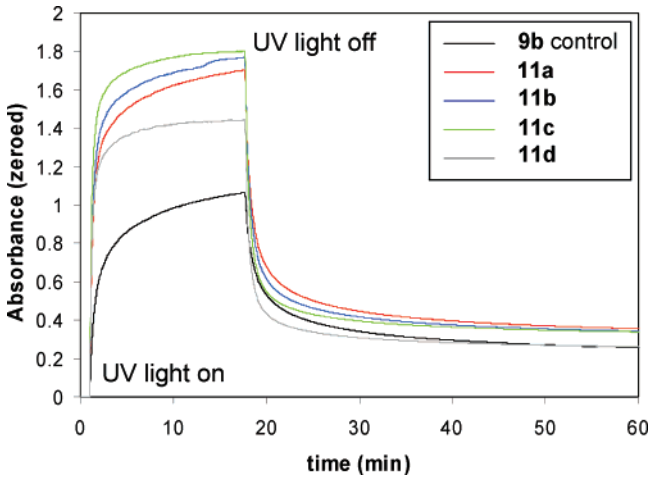

Figure 8. Absorbance vs time for the coloration and decoloration of end-functionalized naphthopyran−poly(*n*-butyl acrylate) conjugates **11a**−**d** and control **9b** in a rigid polymeric host matrix PEGDMA: EBPDMA (1:4). Dye concentration = 1.20×10^{-6} mol/g. Absorbance monitored at λ_{max} of the colored form of the naphthopyran (510 nm). Irradiation at 350−400 nm from 60 to 1000 s (ca. 16.7 min) and decoloration in the dark monitored from 1000 s onward.

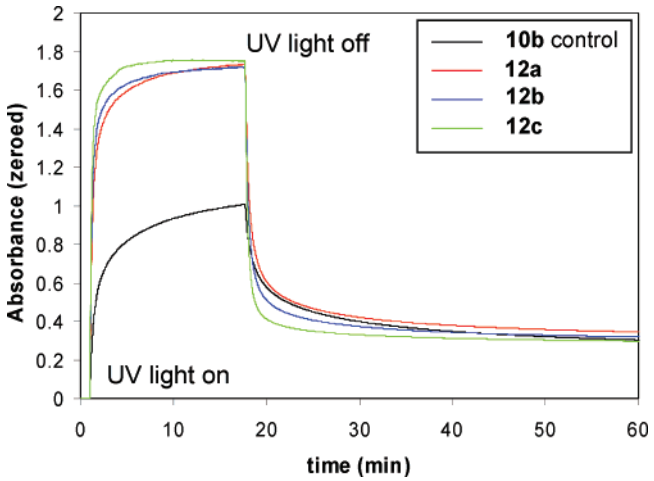

Figure 9. Absorbance vs time for the coloration and decoloration of mid-functionalized naphthopyran−poly(*n*-butyl acrylate) conjugates **12a**−**c** and control **10b** in a rigid polymeric host matrix PEGDMA: EBPDMA (1:4). Dye concentration = 1.20×10^{-6} mol/g. Absorbance monitored at λ_{max} of colored form of the naphthopyran (510 nm). Irradiation at 350−400 nm from 60 to 1000 s (ca. 16.7 min) and decoloration in the dark monitored from 1000 s onward.

influence of these electronic effects in slowing down the fade kinetics of the actual photochromic dye in control **10b** and the corresponding conjugates **12a**−**c**, the effect of conjugate formation with midfunctionalization far outweighs any effects due to this, as reflected in the comparison of fading rates between the two conjugate systems.

As mentioned earlier, naphthopyran photochromics have important application in ophthalmic lenses due to their dark coloration, having large extinction coefficients in the open form, inherent fatigue resistance, and moderately good switching performance. Upon our testing of switching performance, we found that the coloration of the lenses containing end- and mid-functionalized conjugates was about 60 and 70% greater, respectively, than that of the controls after 1000 s irradiation (Figures 8 and 9). Therefore, the attachment of the low T_g poly(*n*-butyl acrylate) tails to the photochromic also greatly improves switching efficiency when the dye conjugate is incorporated within a rigid polymeric host matrix. This has obvious commercial cost benefits in terms of being able to use less photochromic material than otherwise required. Clearly, the polymer conjugation to the naphthopyrans provides superior coloration and decoloration performance by displaying a more square-wave like profile. Coloration of the conjugates reached a steady-state optical density in about 600 s (10 min) whereas that of the control is continuing to rise when irradiation ceased at 1000 s.

Another feature of naphthopyran (chromene) photochromics is that upon exposure to UV radiation there are a number of possible photoisomers of the open form produced.[37−40] With a symmetrically substituted diaryl naphthopyran such as **8** and its derivatives, we expect there to be two major photoisomers. It is known that for one of these photoisomers the thermal reversion back to the closed form is relatively unfavored and requires photobleaching with visible light to progress at any significant rate. This phenomenon is observed in our kinetic experiments (Figures 8 and 9), where the absorbance does not return to a baseline zero value upon decoloration in the dark. A plateau is reached at ca. 18% of the initial absorbance obtained immediately prior to the onset of decoloration, and this appears unaffected by the presence or not of a polymer attached to the dye.

Conclusion

We have shown that the attachment of poly(*n*-butyl acrylate) to naphthopyrans gives markedly improved photochromic performance in coloration and decoloration rates as well as greater optical density in the colored state when in a rigid cross-linked host matrix. In addition, placement of the dye in the middle of a polymer provided greater improvement than at the end. This midfunctionalization was readily achieved by the use of a Y-branching linker based on 3,5-dihydroxybenzoic acid, which enabled the facile synthesis of photochromic dye macroinitiators having two ATRP initiating moieties. Subsequent polymerization from this macroinitiator produced polymer−dye conjugates, where the photochromic dye is positioned in the middle of the polymer. This has provided better encapsulation of the dye for a given molecular weight of the polymer, resulting in faster switching. Logically, three or more polymer chains from the dye may give better performance, but these increases may not outweigh the additional synthetic complexity needed to construct such systems. It is important to note that a inherently slow switching dye will always be a slow switching dye; this general methodology provides the best possible switching environment and works best for those dyes that display a large matrix effect.

Thus, we have extended the parameters available to us in providing indirect control of photochromic performance. Control of a photochromic dye in a rigid matrix via the use of a polymer conjugate can be done through the choice of polymer (low T_g gives faster switching),[11,13] the length of the polymer (the longer the polymer the better the protection from the rigid host matrix),[13] and now the geometry of the polymer (mid placement is more efficient than end placement of the dye).

Experimental Section

Materials. 1,1-Bis(4-methoxyphenyl)prop-2-yn-1-ol[41] and methyl 1,4-dihydroxynaphthalene-2-carboxylate[42] were synthesized using the literature procedures. *n*-Butyl acrylate (99+% purity) was purchased from Aldrich and passed through a column of activated basic alumina immediately prior to use to remove inhibitor. All other reagents were obtained from Aldrich at the highest purity available and used without further purification.

Measurements. Molecular weights and polydispersities of polymers were obtained by gel permeation chromatography (GPC) analyses performed in tetrahydrofuran (THF, 1.0 mL/min) at 25 °C using a Waters GPC instrument, with a Waters 2414 refractive index detector, a series of four Polymer Laboratories PLgel columns (3 × 5 μm Mixed-C and 1 × 3 μm Mixed-E), and Millennium Software. The GPC was calibrated with narrow polydispersity polystyrene standards (Polymer Laboratories EasiCal, MW from 264 to 256 000). ^{1}H and ^{13}C NMR spectra were obtained with a Bruker AV400 or a Bruker AC200 spectrometer. Chemical shifts are reported in ppm from external tetramethylsilane. Monomer conversions were obtained from ^{1}H NMR spectra. The resonances integrated to obtain conversions for *n*-butyl acrylate polymerizations were from the vinyl peaks at 5.86, 6.16, and 6.36 ppm (monomer only) and the OCH_2 peak at 4.14 ppm (monomer and polymer). Positive and negative ion electrospray mass spectra (ESI-MS) were acquired with a VG Platform mass spectrometer using a cone voltage of 50 V with the source maintained at 80 °C. Methanol was used as solvent system with a flow rate of 0.04 mL/min. EI (electron impact) mass spectra were carried out on a ThermoQuest MAT95XL high-resolution mass spectrometer using 70 eV. Photochromic analyses were performed on lenses composed of polymer−photochromic conjugates **11a**−**d** and **12a**−**c** and control species **9b** and **10b** (1.2×10^{-6} mol/g) dissolved in a standard industrial lens formulation of 1:4 weight ratio of poly(ethylene glycol) 400 dimethacrylate (PEGDMA) and 2,2′-bis((4-methacryloxyethoxy)phenyl)propane (EBPDMA) with 0.4% azobis(isobutyronitrile) (AIBN) cured at 80 °C for 16 h. The photochromic response of the lenses were analyzed on a light table (see Supporting Information for schematic representation) comprised of a Cary 50 spectrophotometer and a 300 W Oriel xenon lamp as an incident light source. A series of two filters (Edmund Optics WG320 and Edmund Optics band-pass filter U-340) were used to restrict the output of the lamp to a narrow band (350−400 nm). The samples were monitored at their maximum absorbance of the colored form (510 nm) for a period of 1000 s. Then the decoloration was monitored for a further 4800 s (maximum).

3-(2-Bromoisobutyryloxy)benzoic Acid (4a). *m*-Hydroxybenzoic acid, **1**, (2.0 g, 14.48 mmol) and K_2CO_3 (6.00 g, 43.44 mmol) were dissolved in a mixture of water (18 mL) and *i*-PrOH (6 mL). The solution was cooled in an EtOH/dry ice bath at −20 °C, and to the cold solution was added 2-bromoisobutyryl bromide, **3a**, (3.50 g, 1.88 mL, 15.20 mmol) dropwise over 10 min with vigorous stirring. The mixture was stirred with cooling at −20 °C for an additional 30 min, allowed to warm to 0 °C, and then quenched by the addition of 6 M aqueous HCl (15 mL) [*Caution: foaming*]. After 20 min of stirring at room temperature, the precipitated solid was collected by filtration, washed with water, and dried in a vacuum oven at 40 °C. The product was obtained as a white powder of excellent purity with no further purification required (4.09 g, 98%). ^{1}H NMR (400 MHz, d_6-acetone, δ): 7.98 (d, J = 7.68 Hz, 1H), 7.81 (s, 1H), 7.61 (t, J = 7.68 Hz, 1H), 7.45 (dd, J = 7.68, 1.46 Hz, 1H), 2.10 (s, 6H). ^{13}C NMR (100 MHz, d_6-acetone, δ): 171.54, 167.68, 152.81, 134.11, 131.68, 129.16, 127.65, 124.21, 57.93, 31.67.

3-(Isobutyryloxy)benzoic Acid (4b). *m*-Hydroxybenzoic acid, **1**, (2.0 g, 14.48 mmol) and K_2CO_3 (6.00 g, 43.44 mmol) were dissolved in a mixture of water (18 mL) and *i*-PrOH (6 mL). The solution was cooled in an ice bath, and to the cold mixture was added isobutyryl chloride, **3b**, (1.70 g, 1.67 mL, 15.93 mmol) dropwise over 10 min with vigorous stirring. The mixture was stirred with cooling for an additional 1 h, after which it was quenched by the addition of 6 M aqueous HCl (20 mL) [*Caution: foaming*]. The precipitated solid was collected by filtration, washed with water, and dried in a vacuum oven at 40 °C. The product was obtained as a white powder of excellent purity with no further purification required (2.19 g, 72%). ^{1}H NMR (400 MHz, $CDCl_3$, δ): 12.34 (br s, 1H, OH), 7.99 (d, J = 7.68 Hz, 1H), 7.82 (s, 1H), 7.49 (t, J = 7.68 Hz, 1H), 7.35 (d, J = 7.68 Hz, 1H), 2.84 (septet, J = 6.95 Hz, 1H), 1.34 (d, J = 6.95 Hz, 6H). ^{13}C NMR (100 MHz, $CDCl_3$, δ): 175.36, 171.44, 150.84, 130.72, 129.47, 127.44, 127.19, 123.31, 34.10, 18.81.

3-(2-Bromoisobutyryloxy)benzoyl Chloride (5a). 3-(2-bromoisobutyryloxy)benzoic acid, **4a**, (1.50 g, 5.22 mmol) was added to CH_2Cl_2 (20 mL) together with thionyl chloride (1.86 g, 1.14 mL, 15.67 mmol) and 1 drop of DMF. The mixture was refluxed for 3 h under nitrogen after which the solvent and excess reagent were removed by evaporation in vacuo. Residual thionyl chloride was removed by redissolving the crude product in 1,2-dichloroethane and evaporation of the solvent in vacuo. The product was obtained as a low melting point crystalline solid (yield: quantitative by NMR). ^{1}H NMR (400 MHz, $CDCl_3$, δ): 8.03(d, J = 8.05 Hz, 1H), 7.87 (s, 1H), 7.57 (t, J = 8.05 Hz, 1H), 7.48 (d, J = 8.05 Hz, 1H), 2.08 (s, 6H). ^{13}C NMR (100 MHz, $CDCl_3$, δ): 169.80, 167.36, 150.90, 134.65, 130.04, 128.98, 128.19, 123.84, 54.80, 30.43.

3-(Isobutyryloxy)benzoyl Chloride (5b). This compound was synthesized in an identical manner to that of **5a** from 3-(isobutyryloxy)benzoic acid, **4b**. The product was obtained as a colorless oil (yield: quantitative by NMR). ^{1}H NMR (200 MHz, $CDCl_3$, δ): 7.98 (d, J = 8.04 Hz, 1H), 7.81 (s, 1H), 7.52 (t, J = 8.04 Hz, 1H), 7.40 (d, J = 8.04 Hz, 1H), 2.83 (septet, J = 6.58 Hz, 1H), 1.32 (d, J = 6.58 Hz, 6H). ^{13}C NMR (50 MHz, $CDCl_3$, δ): 175.03, 167.43, 151.03, 134.41, 129.81, 128.69, 128.45, 124.26, 34.02, 18.71.

3,5-Bis(2-bromoisobutyryloxy)benzoic Acid (6a). 3,5-Dihydroxybenzoic acid, **2**, (2.0 g, 12.98 mmol) and K_2CO_3 (8.97 g, 64.90 mmol) were dissolved in a mixture of water (32 mL) and *i*-PrOH (13 mL). The solution was cooled in an EtOH/dry ice bath to −20 °C, and to the cold solution was added 2-bromoisobutyryl bromide, **3a**, (3.04 g, 2.99 mL, 28.55 mmol) dropwise 10 min with vigorous stirring over. The mixture was stirred with cooling at −20 °C for an additional 30 min, allowed to warm to 0 °C, and then quenched by the addition of 6 M aqueous HCl (17 mL) [*Caution: foaming*]. After 20 min of stirring at room temperature, the mixture was extracted with Et_2O. The ethereal extracts were combined, washed with three portions of water, then with brine, and dried with $MgSO_4$. The solvent was evaporated, and the residue was recrystallized from ether/hexane to give a white crystalline solid (4.41 g, 75%). ^{1}H NMR (400 MHz, $CDCl_3$, δ): 10.85 (br s, 1H), 7.80 (d, J = 2.20 Hz, 2H), 7.29 (t, J = 2.20 Hz, 1H), 2.08 (s, 12H). ^{13}C NMR (100 MHz, $CDCl_3$, δ): 170.16, 169.58, 151.11, 131.55, 120.77, 120.22, 54.67, 30.47.

3,5-Bis(isobutyryloxy)benzoic Acid (6b). 3,5-Dihydroxybenzoic acid, **2**, (2.0 g, 12.98 mmol) and K_2CO_3 (8.97 g, 64.90 mmol) were dissolved in a mixture of water (32 mL) and *i*-PrOH (13 mL). The solution was cooled in an ice bath, and to the cold solution was added isobutyryl chloride, **3b**, (3.04 g, 2.99 mL, 28.55 mmol) dropwise over 10 min with vigorous stirring. The mixture was stirred with cooling for an additional 30 min, after which it was quenched by the addition of 6 M aqueous HCl (35 mL) [*Caution: foaming*]. Stirring was continued for another 30 min, and the precipitated solid collected by filtration, washed with water, and dried in a vacuum oven at 40 °C. The

product was obtained as a white powder of good purity with no further purification required (3.02 g, 79%). ^{1}H NMR (400 MHz, $CDCl_3$, δ): 11.49 (br s, 1H, OH), 7.70 (s, 2H), 7.18 (s, 1H), 2.81 (septet, J = 6.95 Hz, 2H), 1.32 (d, J = 6.95 Hz, 12H). ^{13}C NMR (100 MHz, $CDCl_3$, δ): 174.93, 170.40, 151.18, 131.21, 121.00, 120.58, 34.07, 18.74.

3,5-Bis(2-bromoisobutyryloxy)benzoyl Chloride (7a). This compound was synthesized in an identical manner to that of **5a** from 3,5-bis(2-bromoisobutyryloxy)benzoic acid, **6a**. The product was obtained as an oil, which slowly solidified on standing (yield: quantitative by NMR). ^{1}H NMR (400 MHz, $CDCl_3$, δ): 7.82 (d, J = 2.20 Hz, 2H), 7.36 (t, J = 2.20 Hz, 1H), 2.08 (s, 12H). ^{13}C NMR (100 MHz, $CDCl_3$, δ): 169.40, 166.58, 151.27, 135.28, 121.61, 54.51, 30.40.

3,5-Bis(isobutyryloxy)benzoyl Chloride (7b). This compound was synthesized in an identical manner to that of **5a** from 3,5-bis(isobutyryloxy)benzoic acid, **6b**. The product was obtained as a low melting point colorless crystalline solid (yield: quantitative by NMR). ^{1}H NMR (200 MHz, $CDCl_3$, δ): 7.70 (d, J = 2.19 Hz, 2H), 7.25 (t, J = 2.19 Hz, 1H), 2.81 (septet, J = 6.94 Hz, 2H), 1.31 (d, J = 6.94 Hz, 12H). ^{13}C NMR (50 MHz, $CDCl_3$, δ): 174.65, 166.78, 151.34, 134.83, 122.48, 121.49, 34.03, 18.67.

Methyl 6-Hydroxy-2,2-bis(4-methoxyphenyl)-2*H*-naphtho-[1,2-*b*]pyran-5-carboxylate (8). Naphthopyran **8**[33] was synthesized using an alternative literature procedure[43]. A mixture of methyl 1,4-dihydroxynaphthalene-2-carboxylate (1.0 g, 4.58 mmol), 1,1-bis(4-methoxyphenyl)prop-2-yn-1-ol (1.84 g, 6.87 mmol), *p*-toluenesulfonic acid monohydrate (0.13 g, 0.687 mmol), and silica gel (2.5 g) were ground together using a mortar and pestle for 10 min. The mixture was allowed to stand for 1 h after which the product was isolated and purified by column chromatography on silica gel using toluene as the eluent. The solvent was evaporated in vacuo and the resulting red oil treated with a small amount of diethyl ether. The product crystallized very quickly from solution giving a bright yellow solid (0.97 g, 45%). ^{1}H NMR (400 MHz, d_6-acetone, δ): 12.18 (s, 1H), 8.39 (d, J = 8.42 Hz, 1H), 8.31 (d, J = 8.42 Hz, 1H), 7.75 (m, J = 8.42 and 1.46 Hz, 1H), 7.59 (m, J = 8.42 and 1.46 Hz, 1H), 7.48 (d, J = 10.25 Hz, 1H), 7.45 (d, J = 8.78 Hz, 4H), 6.85 (d, J = 8.78 Hz, 4H), 6.32 (d, J = 9.88 Hz, 1H), 4.05 (s, 3H), 3.73 (s, 6H). MS (ES) m/z: 467.5 ($[M - H]^-$).

Naphthopyran Macroinitiator (9a). Methyl 6-hydroxy-2,2-bis(4-methoxyphenyl)-2*H*-naphtho[1,2-*b*]pyran-5-carboxylate, **8**, (1.0 g, 2.13 mmol) was dissolved in dry CH_2Cl_2 (15 mL), and to the solution was added triethylamine (1.10 mL) under argon. 3-(2-Bromoisobutyryloxy)benzoyl chloride, **5a**, (1.30 g, 4.27 mmol) was then added as a solid in one portion, and the mixture stirred at 40 °C for 40 min (reaction progress monitored by TLC). The solvent was evaporated in vacuo, and the residue was redissolved in Et_2O (30 mL) and washed successively with 1M HCl, water, aqueous $NaHCO_3$, water, and brine. The organic layer was dried with $MgSO_4$ and the solvent evaporated in vacuo. The crude product was purified by column chromatography (silica gel, Et_2O/hexane = 2:1) giving a purple-red solid (1.46 g, 93%). ^{1}H NMR (400 MHz, d_6-acetone, δ): 8.46 (d, J = 8.42 Hz, 1H), 8.19 (d, J = 8.05 Hz, 1H), 8.04 (t, J = 1.83 Hz, 1H), 7.89 (d, J = 8.05 Hz, 1H), 7.74 (t, J = 8.05 Hz, 1H), 7.68 (t, J = 8.05 Hz, 1H), 7.57 (m overlap, 2H), 7.47 (d, J = 8.78 Hz, 4H), 7.03 (d, J = 9.88 Hz, 1H), 6.89 (d, J = 8.78 Hz, 4H), 6.43 (d, J = 9.88 Hz, 1H), 3.75 (s, 3H), 3.74 (s, 6H), 2.12 (s, 6H). ^{13}C NMR (100 MHz, d_6-acetone, δ): 171.59, 167.08, 165.69, 161.09, 153.07, 148.08, 141.31, 138.60, 132.52, 132.23, 131.35, 129.94, 129.85, 129.71, 129.12, 128.78, 128.12, 124.76, 124.42, 124.05, 122.53, 121.74, 115.44, 115.34, 84.54, 57.91, 56.49, 53.81, 31.67. MS (EI) m/z: 736.1303 ($C_{40}H_{33}BrO_9$ requires 736.1308).

Naphthopyran Control Compound (9b). This compound was synthesized in an identical manner to that of **9a** using methyl 6-hydroxy-2,2-bis(4-methoxyphenyl)-2*H*-naphtho[1,2-*b*]pyran-5-carboxylate, **8**, and 3-(isobutyryloxy)benzoyl chloride, **5b**. The product was obtained as a purple-red solid (0.218 g, 78%). ^{1}H NMR (400 MHz, d_6-acetone, δ): 8.45 (d, J = 8.42 Hz, 1H), 8.14 (d, J = 8.05 Hz, 1H), 7.98 (t, J = 1.83 Hz, 1H), 7.88 (d, J = 8.05 Hz, 1H), 7.68 (m overlap, 2H), 7.59 (t, J = 8.05 Hz, 1H), 7.53 (dd, J = 8.05 and 1.46 Hz, 1H), 7.47 (d, J = 8.78 Hz, 4H), 7.03 (d, J = 9.88 Hz, 1H), 6.90 (d, J = 8.78 Hz, 4H), 6.43 (d, J = 9.88 Hz, 1H), 3.75 (s, 6H), 3.74 (s, 3H), 2.89 (septet, J = 6.95 Hz, 1H), 1.31 (d, J = 6.95 Hz, 6H). ^{13}C NMR (100 MHz, d_6-acetone, δ): 176.68, 167.11, 165.84, 161.12, 153.34, 148.05, 141.35, 138.63, 132.31, 131.95, 131.36, 129.94, 129.86, 129.82, 129.38, 129.17, 129.13, 128.13, 125.25, 124.45, 124.06, 122.55, 121.79, 115.45, 115.35, 84.55, 56.49, 53.80, 35.67, 20.08. MS (EI) m/z: 658.2207 ($C_{41}H_{34}O_9$ requires 658.2203).

Naphthopyran Macroinitiator (10a). This compound was synthesized in an identical manner to that of **9a** using methyl 6-hydroxy-2,2-bis(4-methoxyphenyl)-2*H*-naphtho[1,2-*b*]pyran-5-carboxylate, **8**, and 3,5-bis(2-bromoisobutyryloxy)benzoyl chloride, **7a**. The product was obtained as a purple-red solid (1.14 g, 59%). ^{1}H NMR (400 MHz, d_6-acetone, δ): 8.46 (d, J = 8.05 Hz, 1H), 8.01 (d, J = 2.20 Hz, 2H), 7.91 (d, J = 8.42 Hz, 1H), 7.69 (t, J = 8.05 Hz, 1H), 7.61 (t, J = 8.05 Hz, 1H), 7.53 (t, J = 2.20 Hz, 1H), 7.47 (d, J = 8.78 Hz, 4H), 7.04 (d, J = 9.88 Hz, 1H), 6.89 (d, J = 8.78 Hz, 4H), 6.43 (d, J = 9.88 Hz, 1H), 3.77 (s, 3H), 3.75 (s, 6H), 2.12 (s, 12H). ^{13}C NMR (100 MHz, d_6-acetone, δ): 171.29, 166.99, 164.96, 161.08, 153.51, 148.20, 141.20, 138.57, 133.31, 131.36, 130.02, 129.90, 129.84, 128.98, 128.13, 124.44, 124.06, 122.72, 122.51, 122.40, 121.58, 115.44, 115.33, 84.55, 57.73, 56.48, 53.91, 31.61. MS (EI) m/z: 900.1 ($C_{44}H_{38}O_{11}Br_2$ requires 900.1).

Naphthopyran Control Compound (10b). This compound was synthesized in an identical manner to that of **9a** using methyl 6-hydroxy-2,2-bis(4-methoxyphenyl)-2*H*-naphtho[1,2-*b*]pyran-5-carboxylate, **8**, and 3,5-bis(isobutyryloxy)benzoyl chloride, **7b**. The product was obtained as a purple-red solid (0.248 g, 78%). ^{1}H NMR (400 MHz, d_6-acetone) δ 8.45 (d, J = 8.42 Hz,1H), 7.89 (m overlap, 3H), 7.69 (t, J = 7.32 Hz, 1H), 7.60 (m, J = 7.32 Hz, 1H), 7.47 (d, J = 9.15 Hz, 4H), 7.40 (t, J = 2.20 Hz, 1H), 7.03 (d, J = 10.25 Hz, 1H), 6.89 (d, J = 8.78 Hz, 4H), 6.43 (d, J = 10.25 Hz, 1H), 3.76 (s, 3H), 3.75 (s, 6H), 2.89 (septet, 2H), 1.31 (d, J = 6.95 Hz, 12H). ^{13}C NMR (100 MHz, d_6-acetone, δ): 176.40, 167.02, 165.25, 161.10, 153.75, 148.13, 141.28, 138.60, 132.79, 131.36, 129.99, 129.85 (shoulder, overlap), 129.85, 129.05, 128.13, 124.45, 124.05, 123.37, 122.60, 122.52, 121.65, 115.45, 115.34, 84.54, 56.49, 53.86, 35.65, 20.01. MS (EI) m/z: 744.2551 ($C_{44}H_{40}O_{11}$ requires 744.2571).

ATRP of *n*-Butyl Acrylate Using Naphthopyran Macroinitiator 9a (11a−d). Five ampoules each containing *n*-butyl acrylate (2.0 g, 15.60 mmol), monofunctionalized naphthopyran macroinitiator, **9a**, (0.1150 g, 0.156 mmol), 4,4′-dinonyl-2,2′-bipyridine (0.1275 g, 0.312 mmol), CuBr (0.0224 g, 0.156 mmol), and benzene (3 mL) were prepared and degassed with four freeze/pump/thaw cycles. The ampoules were sealed and heated at 90 °C in a thermostatted oil bath for various durations. Monomer conversions were determined by ^{1}H NMR analysis of the reaction solution. Excess monomer was then removed

by coevaporation with chloroform using a gentle stream of nitrogen. The resulting crude residues were analyzed by GPC to determine molecular weights and polydispersities. The polymer purification procedure was as follows: (i) polymers were precipitated by dissolution of the crude residues in a minimal volume of CH_2Cl_2 followed by the addition of excess methanol and then slow and partial solvent evaporation (to approximately 3/4 of initial solution volume) using a gentle stream of nitrogen, (ii) the remaining supernatant was decanted, and (iii) solutions of the precipitated polymers in diethyl ether were passed through a short silica column followed by evaporation of the solvent. ^{1}H NMR (**11b**, 200 MHz, d_6-acetone, δ): 8.45 (d, 1H), 8.13 (d, 1H), 8.03 (s, 1H), 7.74−7.52 (m overlap, 4H), 7.47 (d, 4H), 7.03 (d, 1H), 6.90 (d, 4H), 6.43 (d, 1H), 4.37 (m, 1H), 4.07 (br m, polymer butyl CH_2O), 3.77 (s, 6H), 3.74 (s, 3H), 2.36 (br, polymer backbone), 1.92 (br, polymer backbone), 1.64 (br pentet, polymer butyl CH_2), 1.42 (br sextet, polymer butyl CH_2), 0.96 (br t, polymer butyl CH_3).

ATRP of *n*-Butyl Acrylate Using Naphthopyran Macroinitiator 10a (12a−c). Three ampoules each containing *n*-butyl acrylate (4.0 g, 31.21 mmol), bisfunctionalized naphthopyran macroinitiator, **10a**, (0.1404 g, 0.156 mmol), 4,4′-dinonyl-2,2′-bipyridine (0.1275 g, 0.312 mmol), CuBr (0.0224 g, 0.156 mmol), and benzene (2 mL) were prepared and degassed with 4 freeze/pump/thaw cycles. The ampoules were sealed and heated at 90 °C in a thermostatted oil bath for various durations. Monomer conversions were determined by ^{1}H NMR analysis of the reaction solution. Excess monomer was then removed by coevaporation with chloroform using a gentle stream of nitrogen. The resulting crude residues were analyzed by GPC to determine molecular weights and polydispersities. The polymer purification procedure was as follows: (i) polymers were precipitated by dissolution of the crude residues in a minimal volume of CH_2Cl_2 followed by the addition of excess methanol and then slow and partial solvent evaporation (to approximately 3/4 of initial solution volume) using a gentle stream of nitrogen, (ii) the remaining supernatant was decanted, and (iii) solutions of the precipitated polymers in diethyl ether were passed through a short silica column followed by evaporation of the solvent. ^{1}H NMR (**12a**, 400 MHz, d_6-acetone, δ): 8.46 (d, J = 8.4 Hz, 1H), 7.96 (s, 2H), 7.91 (d, J = 8.1 Hz, 1H), 7.71 (t, J = 8.1 Hz, 1H), 7.63 (t, J = 8.1 Hz, 1H), 7.48 (d, J = 8.8 Hz, 4H), 7.41 (s, 1H), 7.05 (d, J = 9.9 Hz, 1H), 6.91 (d, J = 8.8 Hz, 4H), 6.44 (d, J = 9.9 Hz, 1H), 4.38 (br m, 2H), 4.07 (br m, polymer butyl CH_2O), 3.78 (s, 9H), 2.5−2.2 (br, polymer backbone), 1.94 (br m, polymer backbone), 1.64 (br m, polymer butyl CH_2), 1.42 (br m, polymer butyl CH_2), 0.96 (br s, polymer butyl CH_3).

Acknowledgment. The authors thank CSIRO and the CRC for Polymers for their support.

Supporting Information Available: Plots of GPC analyses, plots of $t_{1/2}$ and $t_{3/4}$ vs molecular weight for all conjugates and control compounds, UV−vis absorbance spectra of test lens samples containing compounds **9b**, **11c**, **10b**, and **12b** before and after UV irradiation, schematic representation of experimental setup for the photophysical analysis of test samples. This material is available free of charge via the Internet at http://pubs.acs.org.

References and Notes

(1) Higgins, S. *Chem. Br.* **2003**, *June*, 26−29.
(2) Kawata, S.; Kawata, Y. *Chem. Rev.* **2000**, *100*, 1777−1788.
(3) Yokoyama, Y. *Chem. Rev.* **2000**, *100*, 1717−1739.
(4) Irie, M. *Chem. Rev.* **2000**, *100*, 1685−1716.
(5) Berkovic, G.; Krongauz, V.; Weiss, V. *Chem. Rev.* **2000**, *100*, 1741−1753.
(6) Delaire, J. A.; Nakatani, K. *Chem. Rev.* **2000**, *100*, 1817−1845.
(7) Evans, R. A.; Such, G. K. *Aust. J. Chem.* **2005**, *58*, 825−830.
(8) Evans, R. A.; Hanley, T. L.; Skidmore, M. A.; Davis, T. P.; Such, G. K.; Yee, L. H.; Ball, G. E.; Lewis, D. A. *Nat. Mater.* **2005**, *4*, 249−253.
(9) Evans, R. A.; Such, G. K.; Davis, T. P.; Malic, N.; Lewis, D. A.; Campbell, J. A. Photochromic Compounds Comprising Polymeric Substituents and Methods for Preparation and Use Thereof. WO 2006024099, 2006.
(10) Evans, R. A.; Such, G. K.; Malick, N.; Davis, T. P.; Lewis, D. A. Photochromic Compositions and Articles Comprising Siloxane, Alkylene, or Substituted Alkylene Oligomers. WO 2005105875, 2005.
(11) Such, G. K.; Evans, R. A.; Davis, T. P. *Macromolecules* **2004**, *37*, 9664−9666.
(12) Such, G. K.; Evans, R. A.; Davis, T. P. *Mol. Cryst. Liq. Cryst.* **2005**, *430*, 273−279.
(13) Such, G. K.; Evans, R. A.; Davis, T. P. *Macromolecules* **2006**, *39*, 1391−1396.
(14) Such, G. K.; Evans, R. A.; Davis, T. P. *Macromolecules* **2006**, *39*, 9562−9570.
(15) Such, G. K.; Evans, R. A.; Yee, L. H.; Davis, T. P. *J. Macromol. Sci., Polym. Rev. C* **2003**, *43*, 547−579.
(16) Mantovani, G.; Ladmiral, V.; Tao, L.; Haddleton, D. M. *Chem. Commun.* **2005**, 2089−2091.
(17) Lee, H.; Wu, W.; Oh, J. K.; Mueller, L.; Sherwood, G.; Peteanu, L.; Kowalewski, T.; Matyjaszewski, K. *Angew. Chem., Int. Ed.* **2007**, *46*, 2453−2457.
(18) Zhu, M.-Q.; Zhu, L.; Han, J. J.; Wu, W.; Hurst, J. K.; Li, A. D. Q. *J. Am. Chem. Soc.* **2006**, *128*, 4303−4309.
(19) Zhu, L.; Wu, W.; Zhu, M.-Q.; Han, J. J.; Hurst, J. K.; Li, A. D. Q. *J. Am. Chem. Soc.* **2007**, *129*, 3524−3526.
(20) Fukushima, K.; Vandenbos, A. J.; Fujiwara, T. *Chem. Mater.* **2007**, *19*, 644−646.
(21) Heron, B. M.; Gabbutt, C. D.; Hepworth, J. D.; Partington, S. M.; Clarke, D. A.; Corns, S. N. Rapid Fading Photo-Responsive Materials. WO 2001012619, 2001.
(22) Kumar, A.; VanGemert, B.; Knowles, D. B. Substituted Naphthopyrans. US 5,458,814, 1995.
(23) Coelho, P. J.; Carvalho, L. M.; Abrantes, S.; Oliveira, M. M.; Oliveira-Campos, A. M. F.; Samat, A.; Guglielmetti, R. *Tetrahedron* **2002**, *58*, 9505−9511.
(24) Krishnan, S.; Pyles, R. A.; Johnson, J. B.; Jenkins, M. P.; Pike, T. J. Photochromic Compositions having Improved Fade Rate. US 5,998,-520, 1999.
(25) Misura, M. S.; Kumar, A. Removable Imbibition Composition of Photochromic Compound and Kinetic Enhancing Additive. US 6,-433,043, 2002.
(26) Misura, M. S.; Kumar, A. Removable Imbibition Composition of Photochromic Compound and Epoxy and Polyol Kinetic Enhancing Additives. US 6,713,536, 2004.
(27) Engardio, T. J.; Schlunt, P. D. Photochromic Matrix Compositions for Use in Ophthalmic Lenses. US 6,863,844, 2005.
(28) Becker, R. S.; Michl, J. *J. Am. Chem. Soc.* **1966**, *88*, 5931−5933.
(29) Lenoble, C.; Becker, R. S. *J. Photochem.* **1986**, *33*, 187−197.
(30) VanGemert, B.; Kumar, A.; Knowles, D. B. *Mol. Cryst. Liq. Cryst.* **1997**, *297*, 131−138.
(31) Kumar, A. *Mol. Cryst. Liq. Cryst.* **1997**, *297*, 139−145.
(32) Malic, N.; Evans, R. A. *Aust. J. Chem.* **2006**, *59*, 763−771.
(33) Kumar, A.; VanGemert, B.; Knowles, D. B. Novel Substituted Naphthopyrans. WO 95/16215, 1995.
(34) Gabbutt, C. D.; Hepworth, J. D.; Heron, B. M.; Thomas, D. A.; Kilner, C.; Partington, S. M. *Heterocycles* **2004**, *63*, 567−582.
(35) Zayat, M.; Levy, D. *J. Mater. Chem.* **2003**, *13*, 727−730.
(36) Biteau, J.; Chaput, F.; Boilot, J.-P. *J. Phys. Chem.* **1996**, *100*, 9024−9031.
(37) Delbaere, S.; Luccioni-Houze, B.; Bochu, C.; Teral, Y.; Campredon, M.; Vermeersch, G. *J. Chem. Soc., Perkin Trans. 2* **1998**, 1153−1157.
(38) Coelho, P. J.; Salvador, M. A.; Oliveira, M. M.; Carvalho, L. M. *J. Photochem. Photobiol., A* **2005**, *172*, 300−307.
(39) Sallenave, X.; Delbaere, S.; Vermeersch, G.; Saleh, A.; Pozzo, J.-L. *Tetrahedron Lett.* **2005**, *46*, 3257−3259.
(40) Delbaere, S.; Micheau, J.-C.; Vermeersch, G. *J. Org. Chem.* **2003**, *68*, 8969−8973.
(41) Gabbutt, C. D.; Heron, B. M.; Instone, A. C.; Thomas, D. A.; Partington, S. M.; Hursthouse, M. B.; Gelbrich, T. *Eur. J. Org. Chem.* **2003**, 1220−1230.
(42) Hattori, T.; Harada, N.; Oi, S.; Abe, H.; Miyano, S. *Tetrahedron: Asymmetry* **1995**, *6*, 1043−1046.
(43) Tanaka, K.; Aoki, H.; Hosomi, H.; Ohba, S. *Org. Lett.* **2000**, *2*, 2133−2134.

MA071792L